Colloidal rotation near the colloidal glass transition

Minsu Kim,[1] Stephen M. Anthony,[2] Sung Chul Bae,[3] and Steve Granick[1,2,3,a)]
[1]*Department of Physics, University of Illinois, Urbana, Illinois 61801, USA*
[2]*Department of Chemistry, University of Illinois, Urbana, Illinois 61801, USA*
[3]*Department of Materials Science and Engineering, University of Illinois, Urbana, Illinois 61801, USA*

(Received 28 March 2011; accepted 19 July 2011; published online 5 August 2011)

We compare, using single-particle optical imaging, trajectories of rotation and translation for micron-sized spheres in index-matched colloidal suspensions near their glass transition. Rotational trajectories, while they show intermittent caged behavior associated with supercooled and glassy behavior, explore a sufficiently wider phase space such that in the averaged mean-square angular displacement there appears no plateau regime, but instead sub-Fickian angular diffusion that follows an apparent power law in time. We infer translation and rotation time constants, the former being the time to diffuse a particle diameter and the latter being the time to rotate a full revolution. Correlation between time constants increases with increasing volume fraction, but unlike the case for molecular glasses, the rotation time constant slows more weakly than the translation time. © *2011 American Institute of Physics*. [doi:10.1063/1.3623489]

It is sobering that the quest to understand supercooled and glassy states of liquids, in which viscosity increases by orders of magnitude over a narrow span of a control variable, has lingered for decades as a great unsolved problem in condensed matter physics.[1–3] To point this out is less defeatist than realistic, and the reality is that the longer a problem sits on a research agenda, the more likely it is to suffer from the need for fresh points of view. Here, as experimentalists, we are interested in monodisperse colloidal-sized spherical particles in liquid suspension, which are known to enter jammed glassy states as the volume fraction is raised. They are small enough to undergo Brownian motion, yet large enough to be imaged at the single-particle level in optical microscopes, which present enormous experimental appeal because it eliminates the need for ensemble-averaging that is inherent in nearly all other experimental approaches for studying the glass transition.[4–6] Pioneering single-particle studies, of the same system studied here, previously considered non-Gaussian distribution of displacements in colloid glasses and cooperative motion of the constituent colloidal particles,[7,8] but they did not consider rotation, perhaps because there was no experimental handle by which to do so. Here, capitalizing upon a different experimental approach developed in this laboratory to measure single-particle rotation, we consider translation-rotation correlations in colloidal glasses, for what it is considered to be the first time at the single-particle level.

The rotator phase of plastic crystals, in which atoms rotate freely while locked into position on their crystallographic lattice,[9,10] explains that there is no necessary relation between translation and rotation in condensed matter solids. While it is true that it cannot be quite the same in a colloidal suspension, as viscous damping between neighboring particles would prevent free rotation, to anticipate the same translation-correlations which have, for a long time, been known from classic theories of how dilute particles diffuse in a viscous medium would be physically unreasonable: jamming may likewise retard rotation, and there is also particle-particle friction to consider, perhaps sometimes literal friction when particles jam together, but primarily non-steric hydrodynamic interaction. In the study below, we address these questions quantitatively in the classic "hard sphere" colloidal glass system.

The modulated optical nanoprobes (MOON) particles introduced by Kopelman *et al.*,[11,12] in which rotation is imaged by coating one hemisphere of colloidal particles with metal, were modified here by subsequently coating the metal layer to be chemically nearly identical to that on the other hemispheres, therefore preserving isotropic hard-sphere interactions. We used as parent particles poly-methylmethacrylate (PMMA) spheres with a sterically stabilizing layer of hydroxystearic acid.[13] As stated by the vendor (Dr. Andrew Schofield, The University of Edinburgh, UK) they are 1.42 μm in diameter with ~7% polydispersity. To obtain optical translucency and a good approximation to hard sphere interactions, we followed conventional methods[7,14,15] and dispersed them in a cyclohexylbromide/decalin mixture in a proportion adjusted empirically to match refractive index and density of the swollen particles. MOON tracer particles were prepared by coating, using electron beam deposition onto particles on a planar substrate, 12 nm of aluminum onto the hemisphere not blocked by the substrate. Subsequently, when the tracer particle rotates in suspension by Brownian motion, its image mimics phases of the moon. Earlier, in a study of rotation in dilute suspensions, we described methods to deduce two angles of the tracer particle, θ and ϕ.[16] Here, θ corresponds to full moon orientation, and ϕ to the orientation within the plane of the image, from the perspective of the experimental observer who views the plane.

To prevent selective interaction of the environment with either hemisphere, a polymer (Polymer Source), poly-(styrene-b-acrylic acid), was grafted onto the aluminum

a)Author to whom correspondence should be addressed. Electronic mail: sgranick@uiuc.edu.

coated side such that the acrylic acid attached to the aluminum[17] and polystyrene, a non-adsorbing polymer often used to produce depletion pair potential interaction between PMMA particles,[18] produced steric repulsion with neighboring particles. Microscope images were obtained using bright field microscopy (Zeiss, 160× magnification) and imaged by CCD (Andor IXon), the metal side facing the objective appearing black in the two-dimensional field of view. For the Al coating thickness that we used, the density mismatch gravitational energy, just 0.1 kT, was considered not to affect its rotational mobility (indeed, conventional Au coatings would have been prohibitively dense). In the literature on PMMA particles, the degree to which index-matching solvent might swell particles is a controversial, unsolved matter,[15,19] so here we report particle volume fraction under the assumption that solvent did not swell the particles, recognizing that the actual volume fraction might have been larger by up to 2%–3%.[15] Repeated measurements resulted in a dataset amounting to typically 5–8 trajectories at each volume fraction, with at least five independent MOON particles at each volume fraction.

At the highest volume fraction, where mobility was slowest, single particles were followed for up to 1 week. While one might reasonably wonder whether sample volume fraction remained strictly constant over this long time, and whether sedimentation might confound the measurements, phenomenologically we observed that when evaluating the short-time displacements of trajectories early in the week, and late in the week, they agreed. This we took to indicate that the effects of these sources of potential uncertainty were negligible.

The spatial resolution, determined from the y-intercept of the calculated mean-squared displacements, was better than 50 nm, amounting to 1/2 pixel resolution. Regarding angular displacements, resolution was sufficient to observe 10° changes in the angle (the angle between the two orientation vectors), as determined through linear extrapolation of the mean-squared displacements at short times. The representation of angles in Fig. 1(b) corresponds to a Mercator-style projection of spherical angular space, and as such suffers the usual flaw of cylindrical projections of spheres that rotational distances are not portrayed uniformly. Apparent displacements in ϕ larger than 180° over a single time step were considered to most likely correspond to their shorter 360° complements. Displacements so large that both possibilities must be entertained were rare, only occurring during cage jumps, and as such the effect of this added uncertainty on other portions of the analysis was negligible. In analyzing rotation, we defined clockwise rotation as positive. As rotation was mainly so slow that particles rotated much less than 180° from frame to frame in the data acquisition, we were able to track the direction of rotation.

Trajectories of angular and translational displacement were compared. Consistent with numerous prior studies by others, translational mobility was intermittent: as illustrated in Fig. 1, the illustrative particle's position was at first restricted to a narrow region of space (black line in Fig. 1(a)), then jumped suddenly (red line in Fig. 1(a)) to a new position (blue line in Fig. 1(a)), presumably because of chance collective rearrangements by its neighbors.

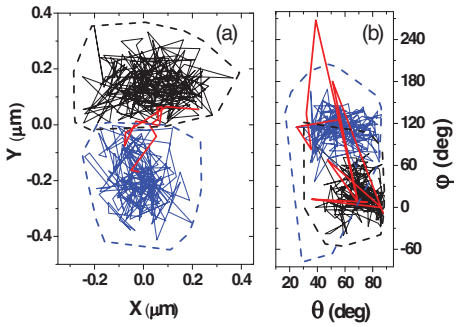

FIG. 1. Typical positional (a) and angular (b) trajectories at the volume fraction of 0.51; the axes are spatial positions x and y (a) and angles θ and φ (b). Here, θ corresponds to full moon orientation and ϕ to the orientation within the plane of the image, from the perspective of the experimental observer who views the plane. Dashed lines are the boundaries of trajectories. The particle jumps from the first cage (black line) to the second cage (blue line) rapidly (red line); here, the red line denoting cage breaking was determined from the large leap in the positional trajectory, but one can also determine it from the angle, as sudden changes in angular trajectory occur simultaneously. The accompanying leaps in angle separate the angular trajectory into two regions, before the leap and after it, but as rotation is not a caged motion, the two regions overlap over longer times. The black solid lines start at −7.5 min, the blue solid lines end at 7.5 min; together the solid lines trace trajectories during 15 min. The dashed lines are boundaries of trajectories during 40 min.

Angular trajectories showed qualitatively similar behavior (Fig. 1(b)). Restricted motion in angular space (black line in Fig. 1(b)) was followed by leaps of angular motion (red line in Fig. 1(b)) at the same time as sudden jumps in translation, landing the particle in a new angular position (blue line in Fig. 1(b)). However, the dashed lines in Fig. 1 show that locations of angular persistence decorrelated more rapidly than those for spatial position. That is, crowding restricted rotation but not for so long as translation, as will be discussed below after first discussing translation-rotation correlations.

The correlation C between translation and rotation, plotted against volume fraction in Fig. 2, was defined as $C = (E[(X_1 - u_1)(X_2 - u_2)])/(\sqrt{E[(X_1 - u_1)^2]} \times \sqrt{E[(X_2 - u_2)^2]})$, where X_1 is the rotational displacement, X_2 is the translational displacement, and u_1 and u_2 are the mean values of X_1 and X_2.[20] It is physically reasonable that C increases from close to zero at low volume fraction to larger levels, rotation becoming increasingly synchronized with translation. More surprising is to notice that C passes through a maximum close to the known glass-transition volume fraction of 0.58,[7,8] and then decreases. An explanation in terms of limited statistics cannot be excluded, given that glassy states are intrinsically non-ergodic.

On the other hand, one can conjecture. It is known that on the approach to the glass or gel transition in colloidal systems, there develops deviations of the van Hove correlation function from Gaussian, and this has been interpreted to stem from transient spatial fluctuations in the local dynamical behavior; in intriguing parallel to the present data, the peak height for the non-Gaussian parameter plotted against lag time increases on the approach to the jamming transition as the system becomes more crowded, then decreases again for the highest volume fractions, thought to be already in the jammed state, for colloidal glass[21] and the colloidal gel.[22] While this non-monotonic behavior of the non-Gaussian parameter has never

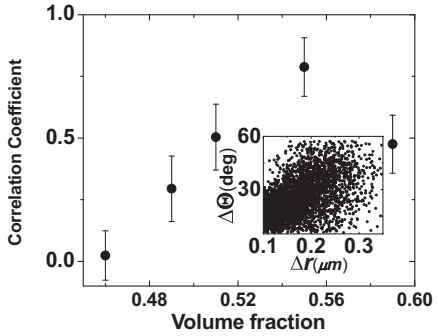

FIG. 2. Correlation coefficient, C, between positional displacement and angular displacement, evaluated over an interval of 3 s, plotted versus volume fraction. Inset illustrates raw data. The choice of 3 s is dictated by the desirability of remaining close to the short time limit of the experiment, as rotation and translation decouple at a long time.

really been explained, one interpretation has been that there is a growing length scale for the heterogeneity as the system becomes crowded, which then decreases again inside the jammed state. While no quantitative explanation is offered at this time, it does seem that when spheres are strongly jammed together, the friction they experience during rotation may become more uniform, and strongest coupling is experienced when the packing between spheres is somewhat less than fully jammed – particles would rotate, when they translate, akin to the manner that balls roll on a plane.

Next, we define rotational relaxation time (τ_R) as the time to rotate 2π rad, and translational relaxation time (τ_T) as the time it takes to diffuse a distance equal to the particle diameter. Plotted against volume fraction in Fig. 3(a), both increase with increasing volume fraction, but the former less strongly so that their ratio decreases, as shown in Fig. 3(b). This short-time limit was determined by the frequency of data acquisition, 1–5 s depending on the experiment.

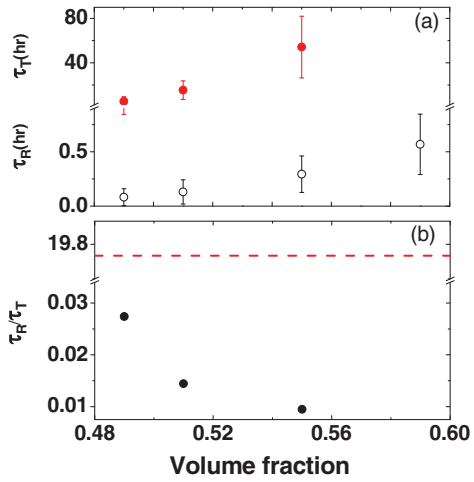

FIG. 3. (a) The rotation (filled symbols) and translation (open symbols) relaxation times are plotted against volume fraction. Rotational relaxation time, τ_R, is defined as the time the particle takes to rotate 2π rad; translational relaxation time, τ_T, as the time to diffuse the particle diameter. (b) The ratio of τ_R to τ_T. Dotted red line is this ratio in dilute suspension. Error bars are standard deviation of independent measurements.

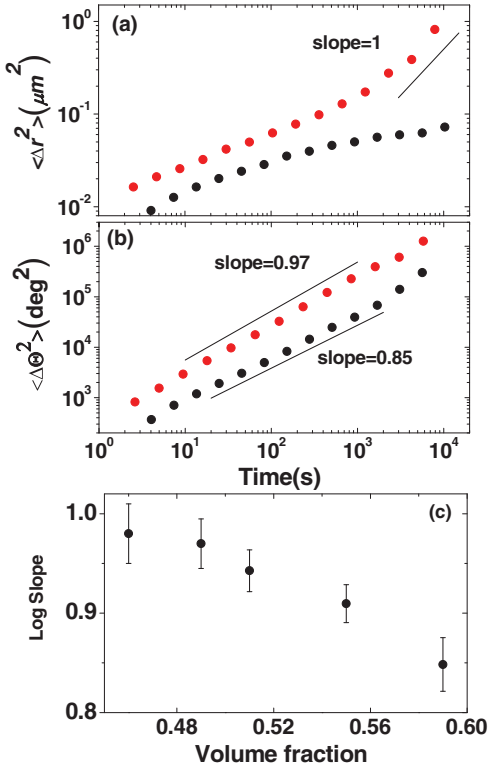

FIG. 4. (a) Positional mean-squared displacement and (b) angular mean-squared displacement are plotted on log-log scales against time at volume fractions 0.49 and 0.59 (red and black circles, respectively). For clarity, only two volume fraction data are shown. (c) The log-log slope decreases monotonically with increasing volume fraction. Error bars are standard deviation of independent measurements.

Note that the ratio of time constants $\tau_R/\tau_T = 19.7$ for an isolated particle in a viscous medium. This is 4 orders of magnitude larger than any value that we observe in this range of crowded volume fractions, which means that particles rotated systematically faster than they translated. This was increasingly so, the higher the volume fraction.

Finally, bearing in mind that mean square translational displacement classically exhibits a subdiffusive-to-diffusive crossover as particles break out of local "cages" at these high volume fractions, we contrast this to mean square angular displacement. First, we confirmed the known classical behavior regarding translation at two volume fractions, the break out to diffusive behavior being observed at the lower volume fraction of 0.49 but not, over the experimental time scale, at the higher volume fraction of 0.59 (Fig. 4(a)). Next, to quantify angular displacement at these same two volume fractions, the equator of each rotating sphere was evaluated as one-dimensional displacement with magnitude $= \sin(\theta) * \Delta\varphi$, and the mean-square angular displacement was plotted against time (Fig. 4(b)). Contrasting strongly with the signature cage behavior for translational motion, the angular mean square displacement, before sufficient time elapses to observe simple diffusive motion, is simply a power law in time. Empirically, the power law slope decreases exponentially with increasing volume fraction (Fig. 4(c)). This may reflect some combination of increasing particle-particle friction, and hydrodynamic interactions analyzed long ago for rotation in di-

lute suspensions.[23] The point in common is that mean-square angular displacement fails to display the plateau "caged" displacement that is classically identified with translational mobility, though it does jump discontinuously when particles shift in position. These differences in the rate-limiting step (steric "caging" by neighbors, for translational diffusion; nonsteric interactions, for angular diffusion) lead naturally to expecting translational and rotational diffusion to decouple, which is what we observe experimentally. This is why, though it is well known that the translation diffusion of the colloidal particles is retarded by the approach to jamming, it is reasonable to find, as we observe, that rotational diffusion is not affected as much.

This differs remarkably from the same distinction in molecular glasses, where rotational diffusion slows in proportion to viscosity increase, but translational diffusion slows by less than this, in some cases less so by up to 2 orders of magnitude, for reasons that have been much discussed.[24–27] Because colloidal rotation is dominated instead by the local friction and hydrodynamic interactions emphasized in this study, it is reasonable that rotational diffusion slows down less steeply, though ultimately a jammed state is likewise reached.

This work was supported by the National Science Foundation, NSF-CBET-0853737. S.M.A. acknowledges the NSF for financial support in the form of a Graduate Research Fellowship. S.C.B. acknowledges funding from a MURI grant through the Army Research Office, W911NF-10-1-0518.

[1]C. A. Angell, Science **267**, 1924 (1995).
[2]M. D. Ediger, C. A. Angell, and S. R. Nagel, J. Phys. Chem. **100**, 13200 (1996).
[3]H. Sillescu, J. Non-Cryst. Solids **243**, 81 (1999).
[4]I. Chang, F. Fujara, B. Geil, G. Heuberger, T. Mangel, and H. Sillescu J. Non-Cryst. Solids **172–174**, 248 (1994).
[5]M. T. Cicerone and M. D. Ediger, J. Chem. Phys. **103**, 5684 (1995).
[6]M. T. Cicerone and M. D. Ediger, J. Chem. Phys. **104**, 7210 (1996).
[7]E. R. Weeks, J. C. Crocker, A. C. Levitt, A. Schofield, and D. A. Weitz, Science **287**, 627 (2000).
[8]W. K. Kegel and A. van Blaaderen, Science **287**, 290 (2000).
[9]J. G. Powles, D. E. Williams, and C. P. Smyth, J. Chem. Phys. **21**, 136 (1951).
[10]M. Godlewska, M. Massalska-Arodz, and S. Urban, Phys. Status Solidi A **73**, 65 (1982).
[11]J. N. Anker and R. Kopelman, Appl. Phys. Lett. **82**, 1102 (2003).
[12]J. N. Anker, C. Behrend, and R. Kopelman, J. Appl. Phys. **93**, 6698 (2003).
[13]L. Antl, J. W. Goodwin, R. D. Hill, R. H. Ottewill, S. M. Owens, S. Papworth, and J. A. Waters, Colloids Surf. **17**, 67 (1986).
[14]E. R. Weeks and D. A. Weitz, Phys. Rev. Lett. **89**, 095704 (2002).
[15]C. P. Royall, R. van Roij, and A. van Blaaderen, J. Phys.: Condens. Matter **17**, 2315 (2005).
[16]S. Anthony, L. Hong, M. Kim, and S. Granick, Langmuir **22**, 9812 (2006).
[17]A. Ulman, Chem. Rev. **96**, 1533 (1996).
[18]A. D. Dinsmore, E. R. Weeks, V. Prasad, A. C. Levitt, and D. A Weitz, Appl. Opt. **40**, 4152 (2001).
[19]L. J. Kaufman and D. A. Weitz, J. Chem. Phys. **125**, 074716 (2006).
[20]R. V. Hogg and E. A. Tanis, *Probability and Statistical Inference*, 7th ed. (Pearson Education, Upper Saddle River, NJ, 2006).
[21]E. R. Weeks, J. C. Crocker, A. C. Levitt, A. Schofield, and D. A. Weitz, Science **287**, 627 (2000).
[22]Y. Gao and M. L. Kilfoil, Phys. Rev. E **79**, 051406 (2009).
[23]V. Degiorgio, R. Piazza, and R. B. Jones, Phys. Rev. E **52**, 2707 (1995).
[24]K. N. Pham, A. M. Puertas, J. Bergenholtz, S. U. Egelhaaf, A. Moussaid, P. N. Pusey, A. B. Schofield, M. E. Cates, M. Fuchs, and W. C. K. Poon, Science **296**, 104 (2002).
[25]Y Gebremichael, M. Vogel, M. N. J. Bergroth, F. W. Starr, and S. C. Glotzer, J. Phys. Chem. B **109**, 15068 (2005).
[26]X. H. Qiu and M. D. Ediger, J. Phys. Chem. B **107**, 459 (2003).
[27]W. K. Kegel and A. van Glaaderen, Science **287**, 290 (2000).